

Hadronic returns to the Z in electron-positron annihilation at high energy

V.A. Khoze^{a,b,1}, D.J. Miller^{c,1}, S. Moretti^{c,1}, and W.J. Stirling^{a,d,1}

*a) Department of Physics, University of Durham,
South Road, Durham DH1 3LE, UK.*

*b) INFN-Laboratori Nazionali di Frascati,
P.O. Box 13, I-00044 Frascati (Rome), Italy.*

*c) Rutherford Appleton Laboratory,
Chilton, Didcot, Oxon OX11 0QX, UK.*

*d) Department of Mathematical Sciences, University of Durham,
South Road, Durham DH1 3LE, UK.*

Abstract

The production of four hadronic jets in e^+e^- collisions above the Z pole is dominated by the QCD $e^+e^- \rightarrow q\bar{q}q\bar{q}, q\bar{q}gg$ processes and, for sufficiently high energy, the electroweak $e^+e^- \rightarrow W^+W^- \rightarrow q\bar{q}q\bar{q}$ process. However there is another mechanism for producing four jets, $e^+e^- \rightarrow Zgg \rightarrow q\bar{q}gg$, which can be regarded as a “hadronic return” to the Z pole. We investigate this new process in detail.

¹E-mails: Valery.Khoze@vxcern.cern.ch; Moretti,D.J.Miller@rl.ac.uk; W.J.Stirling@durham.ac.uk.

1 Introduction and motivation

For e^+e^- centre-of-mass (CM) collision energies above the Z pole, $\sqrt{s} > M_Z$, an important contribution to the cross section for $e^+e^- \rightarrow Z \rightarrow \text{jets}$ comes from the so-called “photonic returns to the Z ”, i.e. events in which one or more photons are emitted by the colliding electron-positron beams prior to the annihilation of the latter into the virtual Z [1]. Such emission can carry away a large fraction of the collider energy, so that the amount left over for the effective e^+e^- interaction, $\sqrt{s_{\text{eff}}}$, can resonate at $\sqrt{s_{\text{eff}}} \approx M_Z$, well below the nominal value of \sqrt{s} . Furthermore, such initial state radiation (ISR) is dominantly collinear to the beam direction, and so many of the photons are in practice not seen by the detectors. At LEP2, with $\sqrt{s} \lesssim 200$ GeV, hadronic events in which $\sqrt{s_{\text{eff}}} \approx M_Z$ have indeed been observed and in fact, because of the resonant shape of the e^+e^- cross section in the vicinity of the Z pole, they constitute a large fraction (about one quarter) of the total e^+e^- production rate. If one wants to study “genuine” physics at the LEP2 collision energy scale one has to remove such events from the analysis. This is also a concern for a future electron-positron linear collider (NLC), where the effect of ISR is a subject of ongoing study [2].

There is another interesting way to return the collider CM energy to the vicinity of M_Z in e^+e^- annihilation. It proceeds via strong (QCD) rather than electromagnetic (EM) interactions. The mechanism is illustrated schematically in Fig. 1a. The virtual Z (or photon) fluctuates into a quark-antiquark loop from which two energetic gluons are emitted. Note that the box diagrams are the only ones that contribute at this leading $\mathcal{O}(e^3 g_s^2)$ order. Triangle diagrams in which the two external gluons are produced via a triple-gluon vertex (see Fig. 1b) are identically zero by colour conservation, and triangle diagrams involving a γ, Z splitting into a pair of on-shell gluons (see Fig. 1c) are forbidden by the Landau-Yang’s theorem. Thus the emission of two gluons from an internal quark loop allows for a reduction of the incoming \sqrt{s} energy of the γ, Z current into a smaller outgoing energy $\sqrt{s_{\text{eff}}}$ of order M_Z , such that an on-shell neutral electroweak (EW) gauge boson can indeed materialise. We may therefore call such events “hadronic returns to the Z ”, or HR for short.

At first sight, the HR cross section would appear to be heavily suppressed compared to the standard EM return. For example, counting powers of coupling constants in the matrix elements squared shows that the former is of order $\mathcal{O}(\alpha_{\text{em}}^3 \alpha_s^2)$ whereas the latter is

of order $\mathcal{O}(\alpha_{\text{em}}^2)$ only. HR events should therefore be a factor of order 10^4 less frequent than photonic return events. Nevertheless it is worth investigating whether the HR events are observable at all at LEP2 and/or NLC. If one continues the simple exercise of coupling counting and multiplies the e^+e^- production cross section at the Z peak, which is of order $\mathcal{O}(\alpha_{\text{em}})$, times $\alpha_{\text{em}}^2\alpha_s^2$, one obtains an estimate for the HR cross section of the order of a few events per hundred inverse picobarn of luminosity at either machine. Since the typical luminosity sample expected at the end of the LEP2 running period is at least of this order of magnitude, HR events may well be already observable. For the NLC, the figure currently foreseen for the yearly luminosity is of the order of 100 fb^{-1} , which could correspond to hundreds of HR events.

Furthermore, the kinematics of HR events is rather peculiar. As no infrared singularities exist in the loop tensor associated with the double gluon emission (see Ref. [3] for a discussion), one expects a clear “ $Z + 2\text{jet}$ ” signal, with the two gluon jets being energetic and quite randomly distributed in the relative angle. The jet–jet invariant mass distribution should be broad, without the low-mass peaking associated with $g^* \rightarrow gg$ for example. In this respect, the HR events could be a sizeable background for processes like $e^+e^- \rightarrow W^+W^- \rightarrow q\bar{q}'Q\bar{Q}'$ and $e^+e^- \rightarrow ZH \rightarrow q\bar{q}b\bar{b}$, the latter when the Z and H masses are degenerate. In both cases, all jets are naturally energetic and well separated. Furthermore, in the second example, the resonant $b\bar{b}$ pair in Zgg events is furnished by the decaying gauge boson, mimicking $H \rightarrow b\bar{b}$.

Of course HR is not the only source of $Z + 2\text{jet}$ events in the Standard Model. The main background (assuming that the Z is clearly identified, for example via its leptonic decays) comes from the $\mathcal{O}(\alpha_{\text{em}}^3)$ $e^+e^- \rightarrow Zq\bar{q}$ process. But here the jet–jet mass distribution is strongly peaked at $M_{jj} \sim 0$ and also, if kinematics allow, at M_Z . A quantitative comparison with HR events will be presented below. If the Z boson in HR events decays to two jets, there is of course a large background from standard QCD and EW $2 \rightarrow 4$ processes [4]. However the topology of such events is in general very different from the HR one, as we shall see.

The discussion so far has been at the level of coupling constants and general kinematics. That, however, is only part of the story. To quantify the above effects one must calculate the appropriate one-loop Feynman diagrams. In fact, it is very difficult to make any *a priori* statements regarding the loop dynamics. Although the expression for the tensor box entering in Fig. 1a, with two massive and two massless external legs, has been known

for a long time [5]² those results cannot be used for the HR cross section calculation here. This is due to the presence of a *Gram determinant* that causes problems with numerical stability when the matrix elements are interfaced with the $1 \rightarrow 3$ phase space. This will be discussed further below.

The paper is organised as follows. In Section 2 we outline how the calculation is performed and make use of the results in order to assess whether hadronic returns induced by the diagrams in Fig. 1a can be of any relevance at all in phenomenological analyses at present and/or future electron-positron colliders. The results presented in Section 3 will help answer this question. In Section 4 we will summarise the main findings of our studies.

2 The calculation

As mentioned in the introduction, the fourth-rank tensor that enters the amplitude squared for $e^+e^- \rightarrow Zgg$ associated with the (six) diagrams in Fig. 1a requires special attention in order to resolve problems with its numerical stability.

As with all calculations at one-loop order, explicit analytic formulae contain determinants in the denominator of the expressions. These determinants can be thought of as arising from the inversion of a set of simultaneous equations, and can be, in general, complicated polynomials of the invariants of the problem. Furthermore, these determinants are raised to a power of up to the rank of the tensor (i.e. in our case, four). Clearly, any analytic expression will be numerically unstable close to the point in phase space where this determinant vanishes. This is the Gram determinant stability problem [8].

In most previous calculations involving triangle and box diagrams this was not significant because the Gram determinant vanished only at the edge of phase space, where the matrix elements diverged anyway due to soft and/or collinear singularities. Indeed this is the case in Refs. [5, 6, 7] where the box diagrams were only required for $2 \rightarrow 2$ processes, ensuring that the determinant singularity was safely stowed away at the edge of phase space. However, when one considers the same box integral for $1 \rightarrow 3$ processes, as we must do here, the Gram determinant singularity now falls in the centre of our phase space and cannot be ignored.

It should be emphasised that this is a purely technical, rather than a conceptual, prob-

²It has also been reproduced in Refs. [6, 7].

lem. There is, in actuality, no physical divergence when the Gram determinant vanishes. It is, in fact, merely an artifact of the way in which the calculation was performed, where the expression is written in a form which makes a *fake* divergence apparent. That is, it should be possible to overcome the Gram determinant problem by either performing the numerical integration at a sufficiently high accuracy or by analytically cancelling by hand divergent terms in the expression to render the matrix elements manifestly finite. However, in the tensor integral of Refs. [6, 7], the Gram determinant in the denominator is raised to the fourth power, giving a divergence which is too powerful to overcome even at quadruple precision. Using this tensor for the $1 \rightarrow 3$ process one would obtain wildly inaccurate results which could not be trusted. Instead one must adopt the second approach and write the matrix elements in a manifestly finite form.

This is not as easy as it sounds. The one-loop matrix elements are extremely complicated and lengthy, containing logarithms, dilogarithms and polynomials of the invariants. It is virtually impossible to find and cancel the divergent terms in such an expression. Instead, we take the approach of Ref. [8], and recalculate the tensor box integral in such a way that these fake Gram determinant singularities are controlled *from the beginning*. In this way we have recalculated the tensor box integral such that it is manifestly finite over all phase space and can be used for $1 \rightarrow 3$ processes without any problems of stability. This method also leads to more compact expressions (although still too lengthy to be reproduced here).

The newly calculated tensor is then interfaced with the incoming $e^+e^- \rightarrow \gamma^*, Z^*$ off-shell current and the outgoing polarisation vectors for the gluons and the gauge boson. In some cases we have kept the latter off-shell, also allowing for contemporaneous γ^*gg and Z^*gg production followed by the decays $\gamma^*, Z^* \rightarrow f\bar{f}$.

The $2 \rightarrow 3$ and $2 \rightarrow 4$ matrix elements (MEs) obtained this way have been integrated numerically over the appropriate three- and four-body phase spaces. Because of delicate cancellations taking place among the diagrams, it is however important to verify the stability of the results against different mappings of the latter. To do so we have implemented the kinematics of the final states both analytically, using different integration variables (see, for example, Ref. [9] for some possible choices), and numerically using the multi-particle phase space generator **RAMBO** [10]. Furthermore, different routines have been used for the numerical integration, namely the Monte Carlo package **VEGAS** [11] and the **NAGLIB** routines **D01EAF** and **D01GCF**. We have found agreement within the numerical errors for all

the resulting outputs. An optimised version of the program designed for high statistics Monte Carlo simulations is available upon request from the authors.

The numerical values for the electroweak and strong parameters used in the numerical calculations presented below are as follows: $\sin^2 \theta_W = 0.2320$, $M_Z = 91.19$ GeV, $\Gamma_Z = 2.5$ GeV, $M_{W^\pm} \equiv M_Z \cos \theta_W \approx 80$ GeV, $\Gamma_{W^\pm} = 2.2$ GeV, $\alpha_{\text{em}} = 1/128$ and α_s is computed at two-loop, with five active flavours and at a renormalisation scale equal to the CM energy. All fermion (i.e. lepton and five quark) masses are set equal to zero. As representative of LEP2 and NLC we have considered CM energies in the range $130 \text{ GeV} \lesssim \sqrt{s} \equiv E_{\text{cm}} \lesssim 500 \text{ GeV}$. Given the value of the top mass, i.e. $m_t \approx 175$ GeV, and the presence of four top propagators in the box diagrams of Fig. 1a, the contribution of the top loop to the overall HR cross section is negligible, both at LEP2 and NLC, and so we do not include it here for simplicity³.

3 Results

We start our investigation of the hadronic returns to the Z by studying the production cross section of the process $e^+e^- \rightarrow Zgg$ as a function of E_{cm} , between typical LEP2 and NLC energies. In order to observe the two gluons as separate jets, one ought to impose some isolation criteria on them. To this end, we simply adopt a jet clustering algorithm [12]: for example, the Durham algorithm [13], with resolution $y_{\text{cut}} = 0.001$. (Note however that none of the main features of our analysis depends upon either the choice of the jet algorithm or of its resolution parameter.) The curve in Fig. 2 reports the production rates with such a di-jet selection enforced.

We see from Fig. 2 that $\sigma(e^+e^- \rightarrow Zgg)$ is very small. The maximum value occurs at $E_{\text{cm}} \approx 280$ GeV, and this is of the order of 0.012 fb only. For typical LEP2 energies, it is always smaller than 0.010 fb, well below detection level. In fact, at least 100 inverse femtobarns of LEP2 luminosity would need to be collected to observe just one such event, a figure which is well beyond the current machine potential. At the NLC, running at around the top-antitop threshold, i.e. with $E_{\text{cm}} \approx 2m_t$, where $m_t = 175$ GeV, the production rate is slightly above 0.010 fb. For 100 fb⁻¹ per year, a handful of $e^+e^- \rightarrow Zgg$ events would be produced at the end of the collider lifetime at such energy (say, of about five years). At

³A similar remark applies to the top loop contribution in the process $gg \rightarrow ZZ$ at LHC [6]. In addition, a non-zero mass in the loop leads to a large proliferation of terms in the tensor reduction, see Ref. [7].

an NLC running at 500 GeV the rates fall back to the values typical of LEP2. However, the order of magnitude of yearly luminosity of a linear collider running with $E_{\text{cm}} \gg 2m_t$ is expected to be not much different from the corresponding value at threshold. Thus some HR events would eventually show up also at an NLC running at high energy.

Figure 2 also shows the cross section for the $\mathcal{O}(\alpha_{\text{em}}^3) e^+e^- \rightarrow Zq\bar{q}$ process. This is *much* larger than the HR cross section, but the kinematics are very different. In fact at CM energies greater than about $2M_Z$ the $Zq\bar{q}$ cross section is completely dominated by the on-shell $ZZ \rightarrow Zq\bar{q}$ contribution, corresponding to final states with $M_{jj} \sim M_Z$. We shall return to this below when we consider kinematic distributions at a typical NLC energy.

The HR cross section values in Fig. 2 seem to contradict the speculations made in the introduction, where we had argued in terms of couplings and kinematics about the possible production rate of $e^+e^- \rightarrow Zgg$ events. In fact our original (optimistic) arguments there are spoiled by the loop behaviour — the far-off-shell internal propagators are an important additional source of suppression. To understand this further we show in Fig. 3 the cross section for $e^+e^- \rightarrow \gamma^*gg$, i.e. for the production of an off-shell photon of virtuality Q_γ , as a function of the latter. For illustrative purposes, we consider a CM energy of 172 GeV. Notice how the cross section decreases by almost two orders of magnitude going from $Q \approx 0$ to $Q \approx M_Z$. Our arguments about the size of the cross section based on counting powers of the coupling did not take this Q dependence into account, and in fact they turn out to be relevant for the small Q limit only. The decrease of available phase space as Q increases is another important factor at this energy.

Having understood the origin of the overall size of the production cross section for $e^+e^- \rightarrow Zgg$, we turn to some typical kinematic distributions of such events at the NLC. The typical energies (momenta) of the two gluons can be seen in the left-hand plot of Fig. 4, whereas in the right-hand plot of the same figure we show the distribution in the momentum of the Z -boson. In Fig. 5, we show instead the invariant mass of the two gluons (upper plot), together with the angular separation between them (lower plot). The distributions shown in these two figures agree remarkably well with the behaviour anticipated in Sect. 1. That is, the two gluons are produced with large energy and with no tendency to be emitted in the same direction (associated with the absence of soft and collinear singularities in the ME). Indeed, in many events the gluons are approximately back-to-back (see lower plot of Fig. 5). Fig. 5 also shows the invariant mass and angular distributions for the $Zq\bar{q}$ process. As anticipated, the former contains a sharp Breit-

Wigner peak at $M_{jj} \sim M_Z$ which is responsible for the bulk of the cross section. The same kinematics are also responsible for the jets being produced at a relative angle of about 60° .

In Figs. 4–5 the default value of 0.001 was used for the resolution parameter y_{cut} of the Durham jet algorithm. However, given the definition of the separation

$$y_{ij} = \frac{2 \min(E_i^2, E_j^2)(1 - \cos \theta_{ij})}{s} \quad (1)$$

which has to be compared to y_{cut} , in terms of the energies E_i and E_j and relative angle θ_{ij} for each pair of particles ij (here, the gg pair only), the kinematics described above imply that there is in fact very little dependence of $\sigma(e^+e^- \rightarrow Zgg)$ on the actual value of y_{cut} . This is illustrated in Fig. 6. If one increases the cut-off by, say, a factor of ten from the default value (0.001), approximately 15% more events are rejected.

So far we have only considered the case of *on-shell* Z boson production. In other words, the rates given so far correspond to what one would obtain by adding together all possible Z decay channels. The dominant among these is of course the decay into $q\bar{q}$ pairs (with a branching ratio of about 70%)⁴, so that the most frequent HR signature is four-jet final states. These are described by the same diagrams as in Fig. 1a, simply supplemented with an additional $Z \rightarrow q\bar{q}$ decay current. In the four-jet channel, now selected by applying the Durham algorithm with cut-off $y_{\text{cut}} = 0.001$ to all *four* partons in the final state, one obtains the typical cross sections of Tab. 1. (Note that we have also included the $\gamma^* \rightarrow q\bar{q}$ propagator in the $2 \rightarrow 4$ HR matrix element.) As already emphasised, the LEP2 four-jet rates are well below detection level. In contrast, the NLC cross sections would still be detectable in the four-jet channel after a few year of running at the level of 100 inverse femtobarns.

However, a more interesting phenomenology could arise from the hadronic returns in the four-jet channel when they manifest themselves in interference processes. In fact, the $q\bar{q}gg$ final state can also be produced at tree-level by the $\mathcal{O}(\alpha_{\text{em}}^2 \alpha_s^2)$ diagrams of Fig. 7. These interfere with those in Fig. 8a⁵. This interference could allow for a more significant effect than the square of the HR amplitudes, possibly even at LEP2 energies, where the QCD process of Fig. 7 is the dominant component of the total four-jet rate (even larger than $e^+e^- \rightarrow W^+W^- \rightarrow q\bar{q}'Q\bar{Q}'$ at small values of y_{cut}).

⁴Here and in the following, we imply a summation over all possible quark flavours in the final states of all reactions we will consider.

⁵To be more precise, only the Abelian graphs do, corresponding to the two gluons produced in a colour singlet state.

However, one should notice that the interference between the diagrams in Fig. 7 and 8a is not the only one occurring at this order of the couplings. In fact, one also has to consider the interference between the tree-level graphs in Fig. 7 and those in Fig. 8b, the latter being nothing more than the former supplemented with the γ, Z self-energy at one-loop (and calculated assuming $\mu = \sqrt{s}$ for the renormalisation scale).

The contributions of these two terms at LEP2 is presented in the upper part of Tab. 2, alongside the leading term given by the square of the tree-level diagrams. For reference, we have set the CM energy equal to 183 GeV. The cross sections are calculated for two illustrative values of y_{cut} in the four-jet regime. From Tab. 2 it can be seen that the interference involving the HR amplitudes is positive and very small, but still an order of magnitude larger than the square of the latter (see Tab. 1). In contrast, the interference involving the self-energy diagrams is negative and sizeable, of the order of 2% of the leading term. From these numbers, we conclude that HR effects are unobservable in practice at LEP2 even in interference processes,. On the one hand, their production rate is tiny *per se*, and on the other hand the other four-jet contributions (including the QCD [14] and EW [15] four-quark $e^+e^- \rightarrow q\bar{q}Q\bar{Q}$ components and their interference [16]) are much larger. In addition the situation is not improved by the next-to-leading order (NLO) QCD corrections to $e^+e^- \rightarrow q\bar{q}gg$ and $e^+e^- \rightarrow q\bar{q}Q\bar{Q}$ [17], which give rise to a K -factor of order 1.5 [18] !

Taking a more optimistic view, we can conclude that at LEP2 hadronic returns do not constitute a serious background to the important physics measurements performed with the four-jet channel. For example, the $W^+W^- \rightarrow$ four jet process is used to measure M_W . Four-jet events can also be generated by the elusive Higgs boson produced in association with a Z , via $e^+e^- \rightarrow ZH \rightarrow q\bar{q}Q\bar{Q}$ (where the second quark pair is dominantly $b\bar{b}$). Had the HR interference effects been sizeable, it would have been a potentially serious background. In fact, by looking at Fig. 9 one realises that not only the $q\bar{q}$ invariant mass induced by the diagrams of Fig. 8a resonates at M_Z ⁶ but also the qg (or, equivalently, $\bar{q}g$) mass has a (negative) Jacobian peak around M_W ! In contrast, the gg distribution (lower plot) would have been of little concern in this respect. The behaviour of the other two four-jet mechanisms discussed is driven by the infrared nature of the QCD interactions (small invariant masses preferred) and by the constraints enforced through the jet-finder,

⁶Further notice that at $E_{\text{cm}} = 183$ GeV a detectable Higgs would have a mass M_H approximately degenerate with that of the Z boson.

with the self-energy contributions being naturally proportional to the tree-level ones.

Notice also that at an NLC with $E_{\text{cm}} = 350$ GeV (see lower part of Tab. 2) hadronic returns do not enter the observable four-jet sample via interference effects. In fact, the corresponding rates are smaller in magnitude than those produced by the HR amplitudes on their own (see Tab. 1), in contrast to the situation at LEP2. The sign is also reversed – the $2 \text{Real}(M_{\text{tree}}M_{\text{returns}}^*)$ contributions are positive in the latter case, and negative in the former.

Finally, for reference, Fig. 10 shows the same three mass distributions discussed in the previous plots but now for the square of the HR matrix element, i.e. $|M_{\text{returns}}|^2$. We again take $E_{\text{cm}} = 183$ GeV and $y_{\text{cut}} = 0.001$ in the Durham algorithm. For comparison, we also present in Fig. 10 the invariant mass of the $q\bar{q}$, $q\bar{Q}$ (or, equivalently, $\bar{q}Q$) and $Q\bar{Q}$ pairs produced in the final state of the Higgs process, when $M_H = M_Z$. Note the overlap of the degenerate Higgs and Z boson mass peaks in the top frame, the latter also appearing in the bottom one (though cut off at the upper edge by phase space constraints on the $e^+e^- \rightarrow ZH$ process) well above the spectrum generated by the squared diagrams of Fig. 8a. The two distributions in the central frame look rather similar. For the $|M_{\text{returns}}|^2$ contributions at the NLC (which we do not reproduce here), the M_{gg} spectrum is basically the same as that given in Fig. 5, the $M_{q\bar{q}}$ one is again a Breit-Wigner centred around M_Z (as in Fig. 10), whereas the M_{qg} one has a Jacobian shape extending to values somewhat higher than those in Fig. 10, having its maximum at about 100 GeV.

4 Summary and conclusions

We have studied in this paper the effects of what we have called “hadronic returns to the Z ” in high-energy e^+e^- annihilation. These correspond to diagrams in which a primary γ, Z current originates a quark loop from which two gluons are emitted in association with a Z boson, the former being energetic enough so that the latter is near its mass-shell. These are a novel source of two-lepton + two-jet and four-jet events which could, *a priori*, constitute a problematic background for W^+W^- and ZH studies at LEP2 and NLC. Naive power counting arguments suggest that the rates could indeed be non-negligible. As there is no substitute for a realistic analysis, we have performed a full matrix element calculation, which has enabled us to compare the HR cross sections with those of the standard processes. We first calculated the hadronic returns as a process

on its own, by integrating the amplitude squared of the relevant perturbative graphs, as well as the interference of these with the tree-level diagrams for quark-antiquark-two-gluon production, corresponding to the case where the Z boson decays into a quark pair.

In every channel studied, the effects of the HR contributions are completely negligible at LEP2. In contrast, at an NLC with energy between 350 and 500 GeV, they can be observed at a rate of a few per 100 inverse femtobarns for various Z decay signatures, whereas their interference with the tree-level contribution to the total four-jet rate is negligible also at the NLC. Thus, the HR contributions are significant enough at such a collider to merit attention when proceeding to experimental studies of high luminosity data samples.

Acknowledgements

SM would like to thank John Hill and the HEP Group at the Cavendish Laboratory (Cambridge) for kindly allowing him to use their computers. SM and DJM are grateful to the Centre for Particle Theory and Grey College at Durham University for their kind hospitality. Discussions with Nigel Glover, Mike Seymour and Jay Watson are gratefully acknowledged. This work was supported in part by the EU IV Framework Programme ‘Training and Mobility of Researchers’, network ‘Quantum Chromodynamics and the Deep Structure of Elementary Particles’, contract FMRX-CT98-0194 (DG 12 - MIHT).

References

- [1] N. Nakanishi, *Progr. Theor. Phys.* **19** (1958) 159;
- D.R. Yennie, S.C. Frautschi and H. Suura, *Ann. Phys.* **13** (1961) 379;
- V.N. Baier and V.A. Khoze, *Sov. Phys. JETP* **21** (1965) 1145;
- E.A. Kuraev and V.S. Fadin, *Sov. J. Nucl. Phys.* **41** (1985) 466;
- F.A. Berends, W.L. van Neerven and G.J. Burgers, *Nucl. Phys.* **B297** (1988) 429;
- Erratum, *ibidem* **B304** (1988) 95;
- G. Altarelli and G. Martinelli, Proceedings of the Workshop ‘*Physics at LEP*’, eds. J. Ellis and R. Peccei, Geneva, 1986, CERN 86-02;
- R. Kleiss, *Nucl. Phys.* **B347** (1990) 29;
- S. Jadach and B.F.L. Ward, *Comp. Phys. Commun.* **56** (1990) 351;
- O. Nicrosini and L. Trentadue, *Phys. Lett.* **B196** (1987) 551; *Z. Phys.* **C39** (1988)

479;

G. Montagna, O. Nicosini and F. Piccinini, *Phys. Lett.* **B406** (1997) 243.

- [2] See, for example, Proceedings of the Workshop ‘ e^+e^- Collisions at 500 GeV. The Physics Potential’, Munich, Annecy, Hamburg, 3–4 February 1991, ed. P.M. Zerwas, DESY 92–123A/B, August 1992, DESY 93–123C, December 1993.
- [3] M.L. Laursen and M.A. Samuel, *Z. Phys.* **C14** (1982) 325.
- [4] See, for example, Proceedings of the Workshop ‘Physics at LEP2’, eds. G. Altarelli, T. Sjöstrand and F. Zwirner, CERN Report 96-01.
- [5] V. Constantini, B. De Tollis and G. Pistoni, *Nuovo Cimento* **2A** (1971) 733.
- [6] E.W.N. Glover and J.J. van der Bij, *Nucl. Phys.* **B321** (1989) 561.
- [7] T. Matsuura and J.J. van der Bij, *Z. Phys.* **C51** (1991) 259;
C. Zecher, T. Matsuura and J.J. van der Bij, *Z. Phys.* **C64** (1994) 219.
- [8] J.M. Campbell, E.W.N. Glover and D.J. Miller, *Nucl. Phys.* **B498** (1997) 397.
- [9] E. Byckling and K. Kajantie, “Particle Kinematics” (John Wiley & Sons, London 1973).
- [10] R. Kleiss, W.J. Stirling and S.D. Ellis, *Comput. Phys. Commun.* **40** (1986) 359.
- [11] G.P. Lepage, *Jour. Comp. Phys.* **27** (1978) 192.
- [12] S. Moretti, L. Lönnblad, T. Sjöstrand, *JHEP* **08** (1998) 001.
- [13] Yu.L. Dokshitzer, contribution cited in Report of the Hard QCD Working Group, Proceedings of the Workshop ‘Jet Studies at LEP and HERA’, Durham, December 1990, *J. Phys.* **G17** (1991) 1537;
N. Brown and W.J. Stirling, *Phys. Lett.* **B252** (1990) 567; *Z. Phys.* **C53** (1992) 629;
S. Catani, Yu.L. Dokshitzer, M. Olsson, G. Turnock and B.R. Webber, *Phys. Lett.* **B269** (1991) 432.
- [14] A. Ballestrero, E. Maina and S. Moretti, *Phys. Lett.* **B294** (1992) 425; *Nucl. Phys.* **B415** (1994) 265.

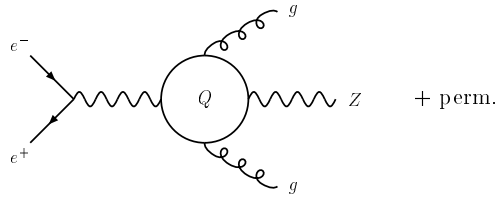
- [15] See, for example, D. Bardin and R. Kleiss (conveners), in Ref. [4], Volume 2, page 3.
- [16] R. Pittau, *Phys. Lett.* **B335** (1994) 490.
- [17] E.W.N. Glover and D.J. Miller, *Phys. Lett.* **B396** (1997) 257;
J.M. Campbell, E.W.N. Glover and D.J. Miller, *Phys. Lett.* **B409** (1997) 503;
Z. Bern, L. Dixon, D.A. Kosower and S. Weinzierl, *Nucl. Phys.* **B489** (1997) 3;
Z. Bern, L. Dixon, D.A. Kosower, *Nucl. Phys.* **B513** (1998) 3.
- [18] A. Signer and L. Dixon, *Phys. Rev. Lett.* **D78** (1997) 811; *Phys. Rev.* **D56** (1997) 4031;
A Signer, *Comp. Phys. Commun.* **106** (1997) 25;
Z. Nagy and Z. Trócsányi, *Phys. Rev. Lett.* **79** (1997) 3604; *Phys. Rev.* **D59** (1999) 014020; *Phys. Rev.* **D57** (1998) 5793;
J.M. Campbell, M.A. Cullen and E.W.N. Glover, preprint DTP-98-58, September 1998, [hep-ph/9809429](https://arxiv.org/abs/hep-ph/9809429).

$\sigma(e^+e^- \rightarrow \gamma^*/Z^*gg \rightarrow q\bar{q}gg)$ (pb)					
E_{cm} (GeV)					
136	161	172	183	192	205
9.9×10^{-7}	1.3×10^{-6}	1.5×10^{-6}	1.8×10^{-6}	1.9×10^{-6}	2.1×10^{-6}
350			500		
2.7×10^{-6}			2.1×10^{-6}		
Durham scheme			$y_{\text{cut}} > 0.001$		

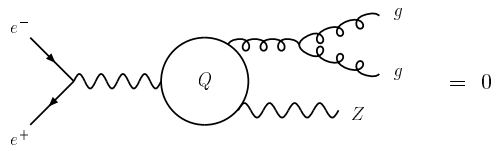
Table 1: Cross sections for the hadronic returns in the four-jet channel at eight different energy points representative of the LEP2 (upper) and NLC (lower) colliders. The jet clustering algorithm used to separate four jets is the Durham algorithm, with cut-off parameter $y_{\text{cut}} > 0.001$. A summation over all possible quark flavours in the final state has been performed. The numerical errors do not affect the significant digits shown.

$\sigma(e^+e^- \rightarrow q\bar{q}gg)$ (pb)			
$E_{\text{cm}} = 183$ GeV			
y_{cut}	$ M_{\text{tree}} ^2$	$2 \text{ Real}(M_{\text{tree}}M_{\text{self}}^*)$	$2 \text{ Real}(M_{\text{tree}}M_{\text{returns}}^*)$
0.001	+5.73	-0.13	+0.0000089
0.010	+0.54	-0.012	+0.0000047
$E_{\text{cm}} = 350$ GeV			
y_{cut}	$ M_{\text{tree}} ^2$	$2 \text{ Real}(M_{\text{tree}}M_{\text{self}}^*)$	$2 \text{ Real}(M_{\text{tree}}M_{\text{returns}}^*)$
0.001	1.09	-0.020	-0.00000019
0.010	0.10	-0.0019	-0.00000084
Durham scheme			

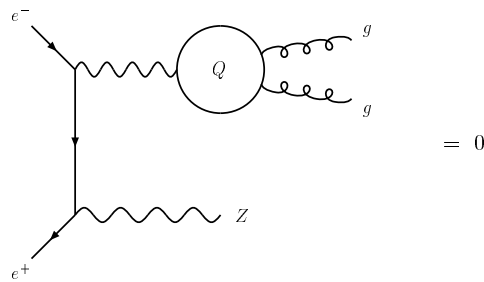
Table 2: Cross sections for the three sources of two-quark-two-gluon events defined in the text: $|M_{\text{tree}}|^2$, $2 \text{ Real}(M_{\text{tree}}M_{\text{self}}^*)$ and $2 \text{ Real}(M_{\text{tree}}M_{\text{returns}}^*)$, for two representative values of the cut-off y_{cut} . The jet clustering algorithm used to separate the four jets is the Durham algorithm. The CM energies are 183 and 350 GeV, as representative of LEP2 and NLC. A summation over all possible quark flavours in the final state has been performed. The numerical errors do not affect the significant digits shown.



(a)



(b)



(c)

Figure 1: Lowest order diagrams responsible for the $e^+e^- \rightarrow Zgg$ process. An internal wavy line represents a γ or a Z . Permutations are not shown. Graphs (a) are the hadronic returns. Graphs (b) and (c) are prohibited, as discussed in the text.

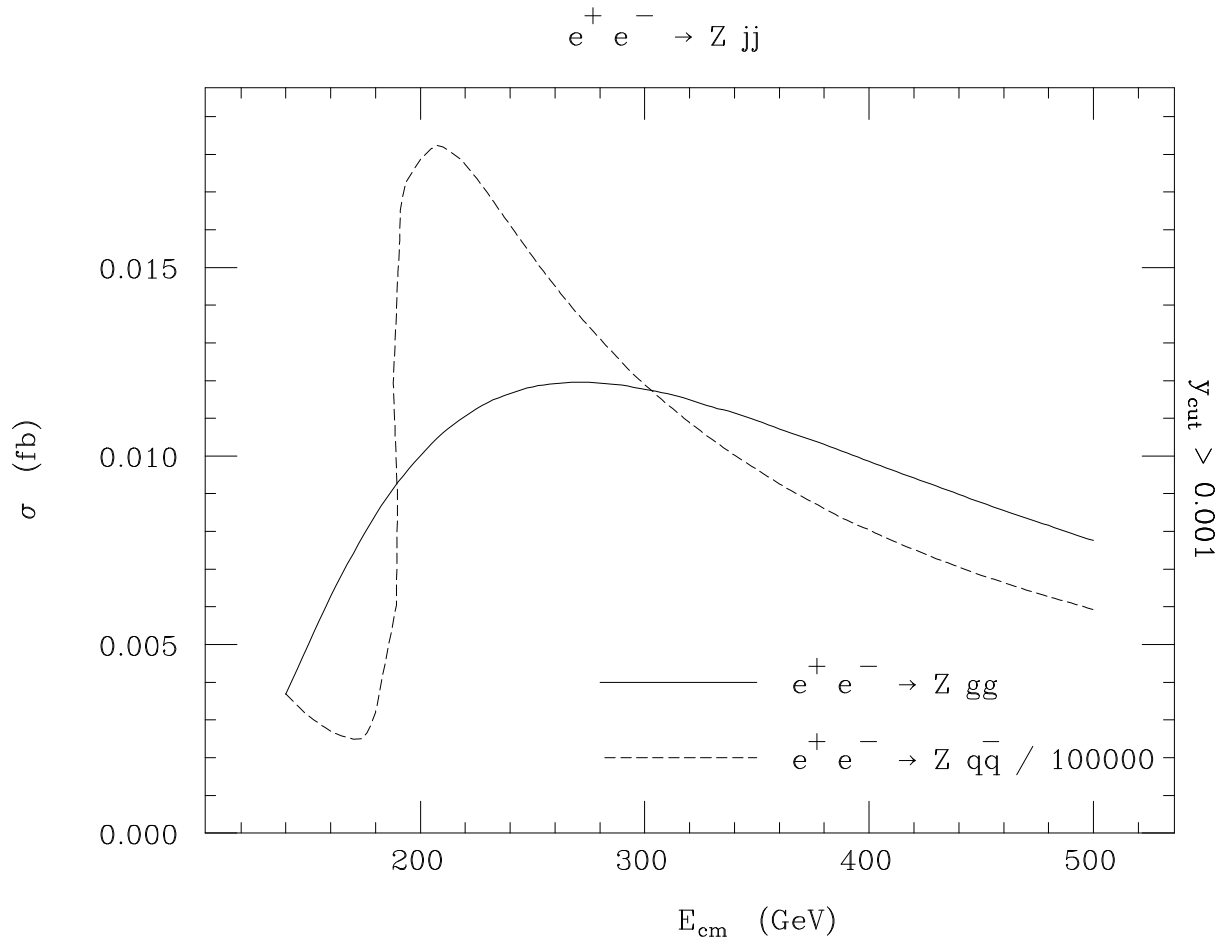


Figure 2: Cross section for $e^+e^- \rightarrow Zgg$ events as a function of the CM energy. The jet clustering algorithm used to separate the gluon jets is the Durham algorithm, with cut-off $y_{\text{cut}} > 0.001$. Also shown is the EW $e^+e^- \rightarrow Zq\bar{q}$ cross section, scaled by a factor of 10^{-5} .

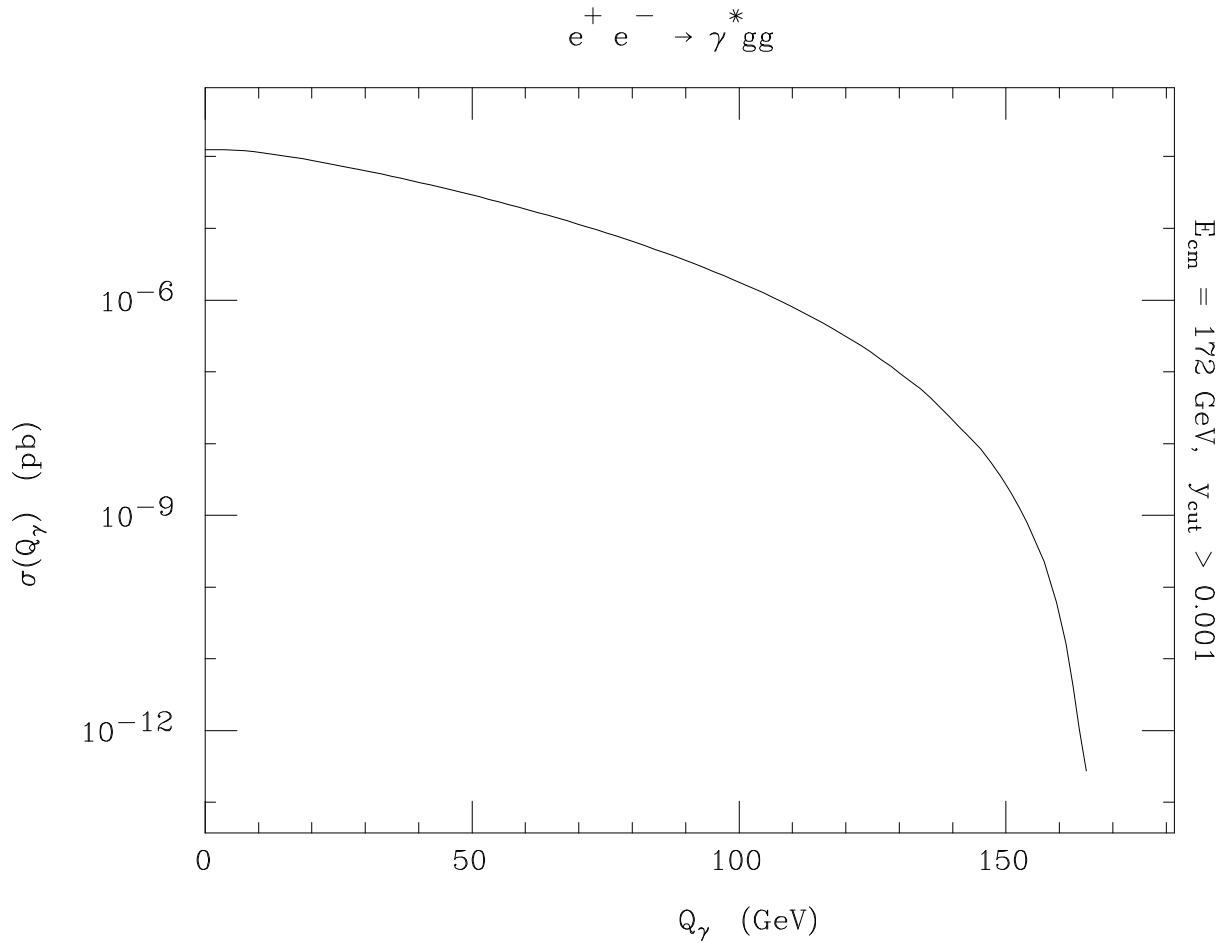


Figure 3: Cross section for $e^+e^- \rightarrow \gamma^*gg$ events as a function of the photon virtuality Q_γ at $E_{\text{cm}} = 172 \text{ GeV}$. The jet clustering algorithm used to separate the gluon jets is the Durham one, with cut-off $y_{\text{cut}} > 0.001$.

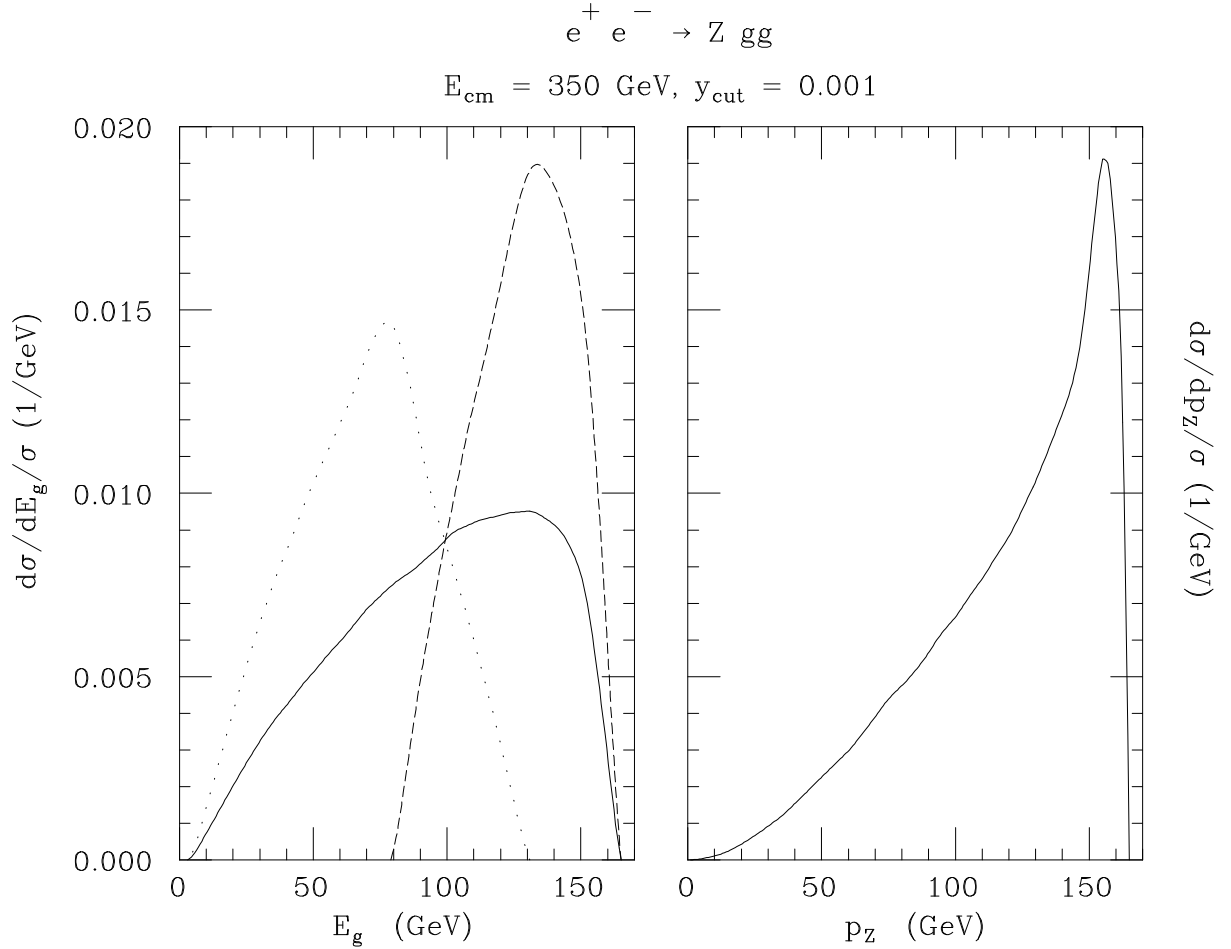


Figure 4: Differential distributions in the gluon energy (left: solid for any of the gluons and dashed[dotted] for the most[least] energetic one) and in the Z momentum (right) for $e^+e^- \rightarrow Zgg$ events at $E_{\text{cm}} = 350 \text{ GeV}$. The jet clustering algorithm used to separate the gluon jets is the Durham algorithm, with cut-off $y_{\text{cut}} > 0.001$. Normalisation is to unity.

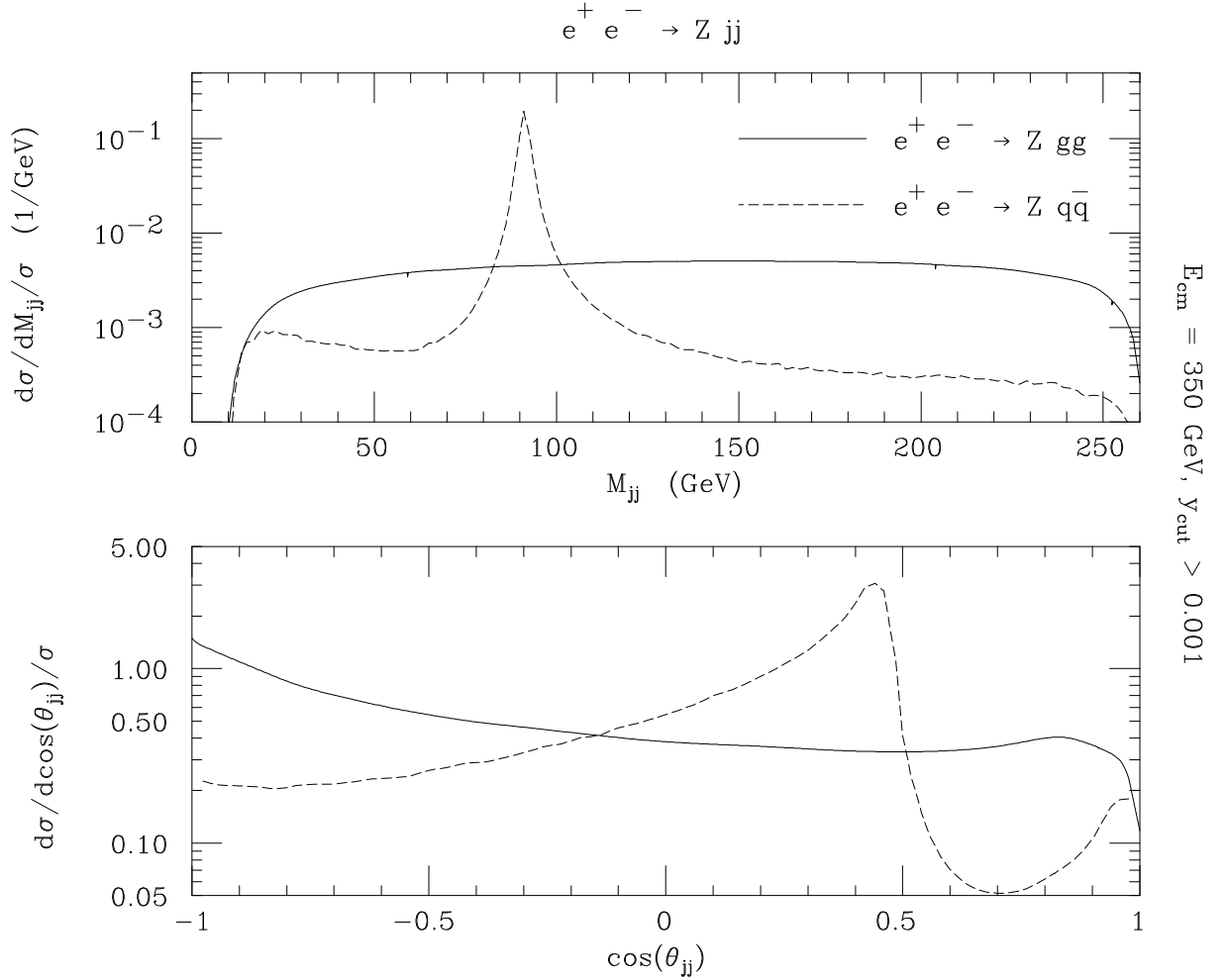


Figure 5: Differential distributions in the gluon-gluon invariant mass (upper plot) and relative cosine (lower plot) for $e^+e^- \rightarrow Zgg$ events at $E_{\text{cm}} = 350 \text{ GeV}$. The jet clustering algorithm used to separate the gluon jets is the Durham algorithm, with cut-off $y_{\text{cut}} > 0.001$. Normalisation is to unity. Also shown are the corresponding distributions for the EW $e^+e^- \rightarrow Zq\bar{q}$ process.

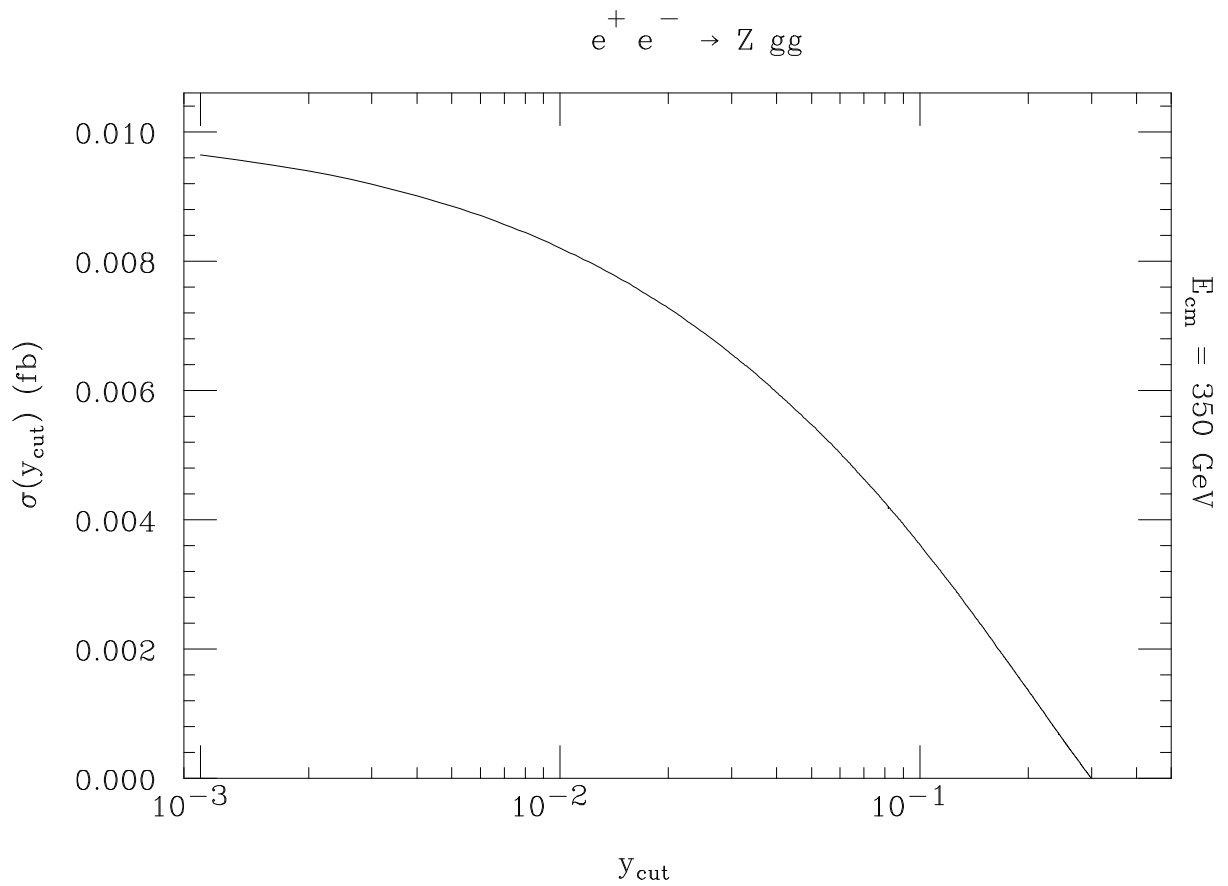


Figure 6: HR cross section as a function of the cut-off y_{cut} in the Durham jet algorithm for $e^+e^- \rightarrow Zgg$ events at $E_{\text{cm}} = 350$ GeV.

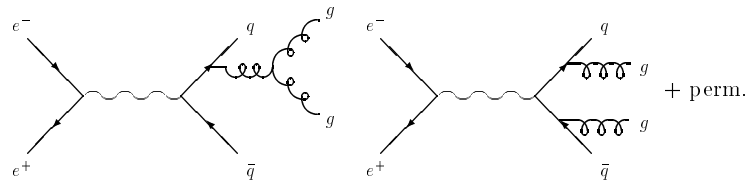


Figure 7: Representative Feynman diagrams contributing in lowest order to $e^+e^- \rightarrow q\bar{q}gg$. An internal wavy line represents a γ or a Z . Permutations are not shown.

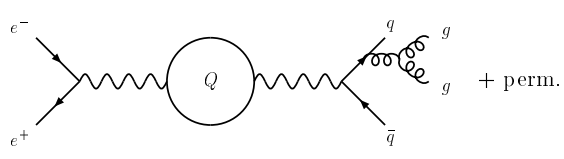
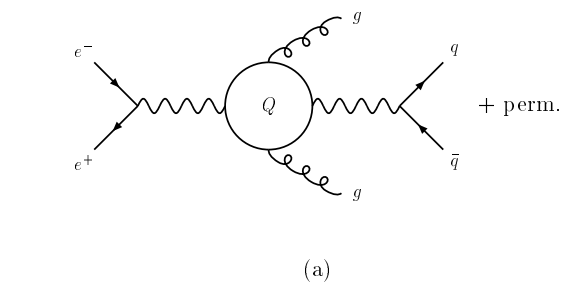


Figure 8: Representative Feynman diagrams contributing in lowest order to the process $e^+e^- \rightarrow q\bar{q}gg$ via one quark loop at order $\mathcal{O}(\alpha_{\text{em}}^4 \alpha_s^2)$. An internal wavy line represents a γ or a Z . Permutations are not shown. Graphs (a) are the hadronic returns. Graphs (b) are the γ/Z self-energies.

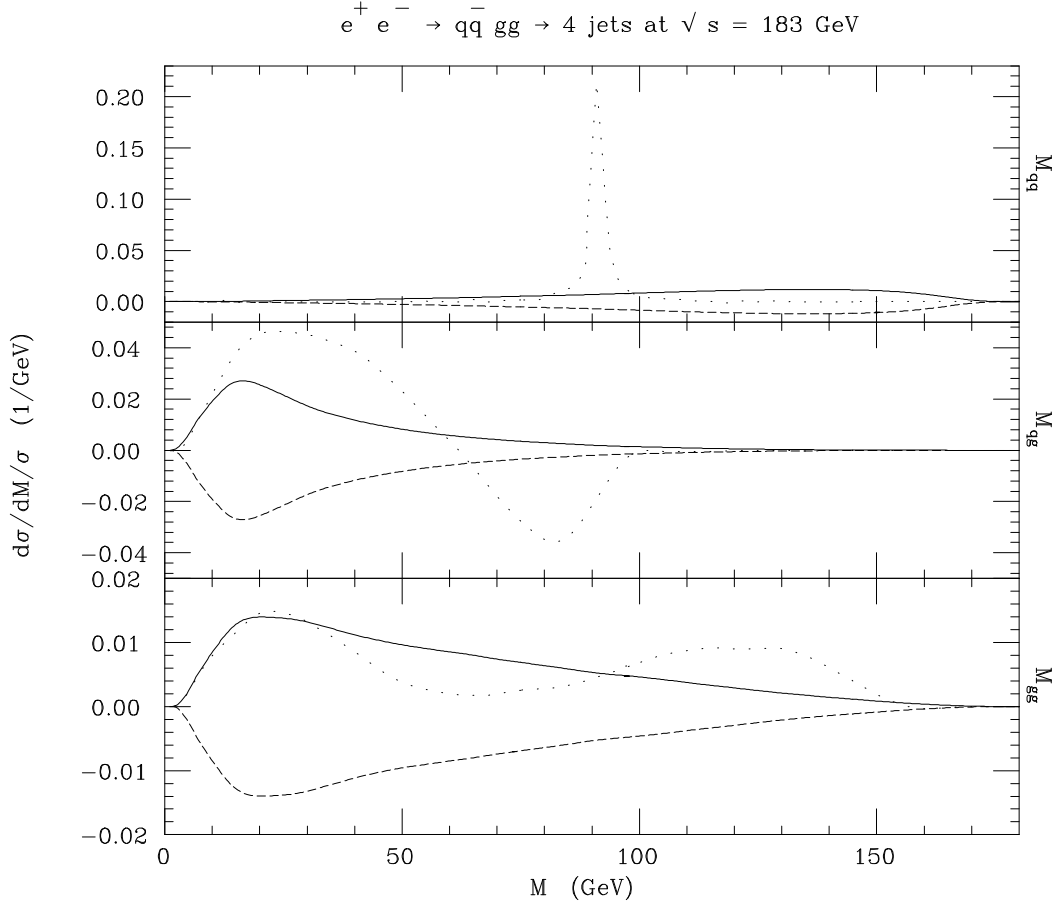


Figure 9: Differential distributions in the invariant mass of the $q\bar{q}$ (upper frame), qg (central frame) and gg (lower frame) pairs for the three sources of two-quark-two-gluon events defined in the text: $|M_{\text{tree}}|^2$ (solid); $2 \text{ Real}(M_{\text{tree}}M_{\text{self}}^*)$ (dashed); $2 \text{ Real}(M_{\text{tree}}M_{\text{returns}}^*)$ (dotted). The CM energy is 183 GeV. The jet clustering algorithm used to separate four jets is the Durham algorithm, with cut-off $y_{\text{cut}} > 0.001$. A summation over all possible quark flavours in the final state has been performed. Normalisation is to unity.

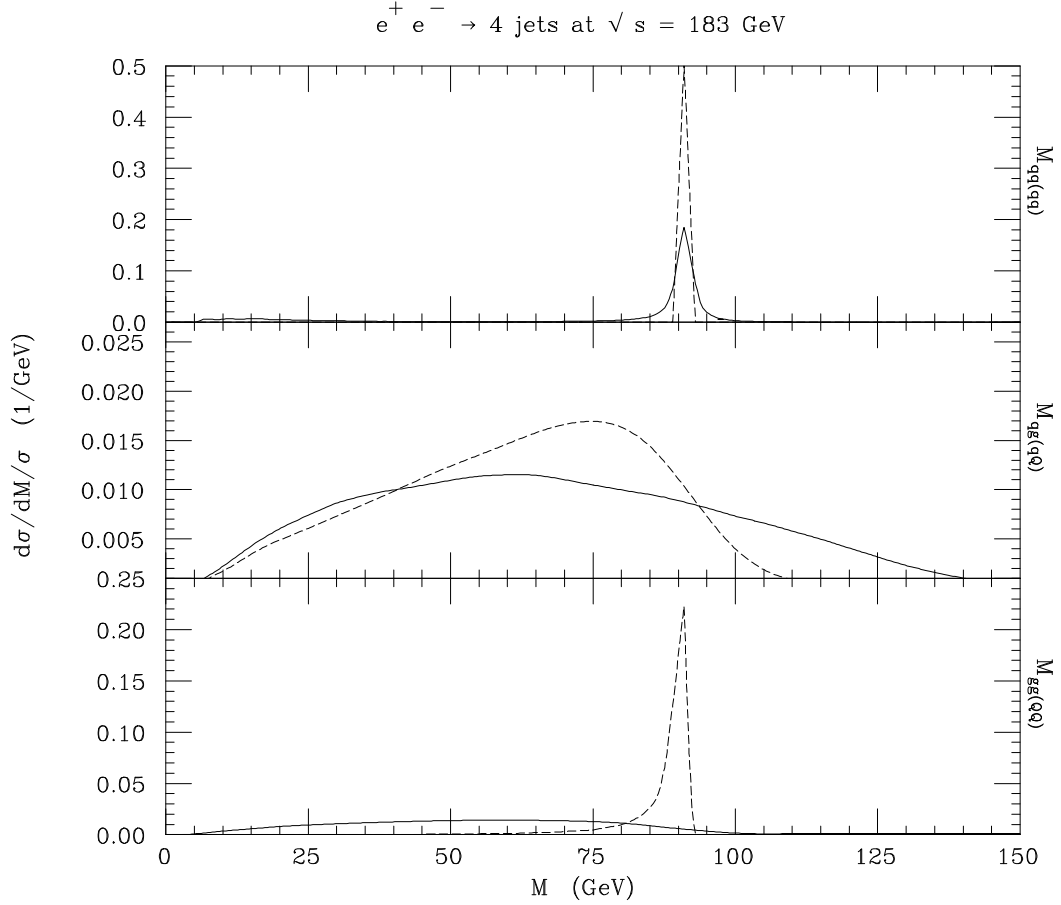


Figure 10: Differential distributions in the invariant mass of the $q\bar{q}(q\bar{q})$ (upper frame), $qg(q\bar{Q})$ (central frame) and $gg(Q\bar{Q})$ (lower frame) pairs for the two processes: $e^+e^- \rightarrow Z, \gamma^* gg \rightarrow q\bar{q}gg$ (solid) and $e^+e^- \rightarrow HZ \rightarrow q\bar{q}Q\bar{Q}$ (dashed). The CM energy is 183 GeV. The jet clustering algorithm used to separate four jets is the Durham algorithm, with cut-off $y_{\text{cut}} > 0.001$. A summation over all possible quark flavours in the final state has been performed. Normalisation is to unity.